اولین کنفرانس احتراق ایران
بهمن ماه ۱۳۸۴- تهران - دانشگاه تربیت مدرس
انجمن احتراق ایران

Relative roles of temperature and fuel concentration in single-step and two-step soot formation models

Iman Zahmatkesh[1], Mohammad Moghiman[2]
Faculty of Mechanical Engineering, Ferdowsi University of Mashhad, Mashhad, Iran
I_Zahmat@yahoo.com

Abstract

This paper presents a comparison between the roles of fuel concentration and temperature distributions in the prediction of three widely used single-step and two-step soot formation models. The single-step soot models calculate soot formation directly while the two-step model computes soot through the formation of nuclei radicals. The comparison is carried out numerically in a turbulent spray flame. In order to model the reactive flowfield, a hybrid Eulerian-Lagrangian method is employed. Equations governing the gas phase are solved by a control-volume based semi-implicit iterative procedure while the time-dependent differential equations for fuel droplets are integrated by a semi-analytic method. The results reveal that the role of fuel concentration is higher than temperature in the Khan's single-step model. The results also show that in the Edelman's single-step model and the two-step model, the roles of temperature in the process of soot formation are inadequately exaggerated. By increasing the role of fuel concentration on soot formation, a new version of the two-step model is proposed whichmakes the best agreement with experimental data.

Keywords: soot formation model- temperature- fuel concentration- spray flame.

1- Introduction

Due to the extremely small size of soot, it can be inhaled deeply into the lungs and its removal from the human air supply through filtering is difficult. Thus, it is widely acknowledged that soot is detrimental to human health. As a result, efforts have been devoted to study the process leading to soot and to find mathematical models which correctly predict soot formation. It is well documented that there are two parameters which mainly affect the formation of soot that are the distributions of fuel concentration and temperature.As a result, all of the soot models have been proposed until now consider a combination of these two parameters for their mathematical equation for the rate of soot formation. The matter which is not studied up to here is the examination of the relative roles of fuel concentration and temperature in the soot formation models. The matter seems to be of great importance since the special conditions of the flame in which a soot model has been derived can strongly affect the relative role of fuel concentration and temperature distributions in the soot formation model which in turn may leads to incorrect predictions in other types of flames.

The aim of the present work is a comparison between the roles of fuel concentration and temperature distributions in the prediction of three widely used single-step and two-step soot formation models. The single-step soot models calculate soot formation directly while the two-step model computes soot through the formation of nuclei radicals. Having a high soot concentration can help to the effect different parameters in the formation of soot be highlight. Thus, in this investigation a turbulent spray flame is chosen for the study. For each of the three soot model, the relative roles of fuel concentration and temperature distributions are assessed and their sensitivities are addressed with respect to fuel concentration and temperature distributions.

2- Theoretical formulation

2-1- Physical system and assumptions

The physical system refers to the evaporation and combustion of a continuously injected liquid fuel spray in a combustor. The air enters the combustor with a swirl while the liquid fuel is sprayed on it. The following assumptions have been made in the present study:

i. The fuel spray is considered to consist of finite size ranges, with the size distribution specified by the Rosin–Rammler function.
ii. A one-way interaction model is used for the gas flow and droplets trajectory analysis. That is, it is assumed that air carries the droplets, but they have no effect on the air flow.
iii. Buoyancy forces are neglected.

---

1 - M. Sc.
2 - Professor

iv. Virtual mass force and Basset force on liquid droplets are not considered due to high-density ratio between the phases.
v. There is no nucleation, collision, break-up, coagulation, or micro-explosion of droplets.
vi. Droplets do not take part in radiative energy exchange.
vii. Fuel is considered to be cetane.

2-2- Numerical model

The numerical model is based on a typical Eularian gas phase and Lagrangian droplet phase formulation. Since a one-way interaction model is used for the gas flow and droplet trajectory analysis, the air flowfield is first evaluated and the results are used for evaluation of the droplet trajectories.

2-2-1- Gas phase conservation equations

The average gas phase equations are as follows:

Continuity:

$$\frac{\partial u}{\partial x}+\frac{1}{r}\frac{\partial}{\partial r}(rv)=\dot{S} \tag{1}$$

Momentum:

$$\frac{1}{r}\left[\frac{\partial}{\partial x}(r\rho uu)+\frac{\partial}{\partial r}(r\rho uv)\right]=-\frac{\partial p}{\partial x}+\mu\nabla^2 u-\frac{1}{r}\frac{\partial}{\partial r}(r\rho\,\overline{u'v'})-\frac{\partial}{\partial x}(\rho\,\overline{u'u'}) \tag{2}$$

$$\frac{1}{r}\left[\frac{\partial}{\partial x}(r\rho uv)+\frac{\partial}{\partial r}(r\rho vv)-\rho w^2\right]=-\frac{\partial p}{\partial r}+\mu(\nabla^2 v+\frac{v}{r^2})-\frac{1}{r}\frac{\partial}{\partial r}(r\rho\,\overline{v'v'})-\frac{\partial}{\partial x}(\rho\,\overline{u'v'})-\frac{1}{r}\rho\,\overline{w'w'} \tag{3}$$

$$\frac{1}{r}\left[\frac{\partial}{\partial x}(r\rho uw)+\frac{\partial}{\partial r}(r\rho vw)+\rho vw\right]=\mu(\nabla^2 w-\frac{w}{r^2})-\frac{1}{r}\frac{\partial}{\partial r}(r\rho\,\overline{v'w'})-\frac{\partial}{\partial x}(\rho\,\overline{u'w'})-\frac{1}{r}\rho\,\overline{v'w'} \tag{4}$$

Where, u, v, and w are the axial, radial, and tangential velocity components, respectively. Also, r is the radial direction and x is the axial direction. $\dot{S}$ is the gas phase mass source term due to evaporation of fuel droplets and p is pressure.

In the view of inability of the $k-\varepsilon$ model to cope with anisotropic flows [1], the turbulent stresses are calculated from an algebraic stress model [2]. Also, a conventional wall-function approach is used in the near-wall region to bridge the viscous sublayer in such a way that the first grid points from the walls be located in the region where $16\le y^+\le 50$.

Energy:

$$\frac{1}{r}\left[\frac{\partial}{\partial x}(r\rho uh)+\frac{\partial}{\partial x}(r\rho vh)\right]=\Gamma_h\nabla^2 h-\frac{1}{r}\frac{\partial}{\partial r}(r\rho\,\overline{v'h'})-\frac{\partial}{\partial x}(\rho\,\overline{u'h'})+\dot{S}_h \tag{5}$$

Here, h is enthalpy. The energy source term ($\dot{S}_h$) has two components. One of which is the net energy absorbed by the exchange of radiation which is evaluated from Gosman and Lockwood [3]:

$$\dot{S}_h=2a\times\left[R_x+R_r-2E_b\right] \tag{6}$$

Where, E_b is the black body radiation. Here, R_x and R_r are the axial and radial radiant fluxes which are determined by the solution of two differential equations:

$$\frac{d}{dx}\left[\Gamma_x\frac{dR_x}{dx}\right]+a(E_b-R_x)+\frac{s}{4}(R_r-R_x)=0 \tag{7}$$

$$\frac{1}{r}\frac{d}{dx}\left[r\left(\Gamma_r\frac{dR_r}{dx}\right)\right]+a(E_b-R_x)+\frac{s}{4}(R_r-R_x)=0 \tag{8}$$

Where, a and s are absorption and scattering coefficients, respectively.

The second component in the energy source term is the energy generated due to chemical reaction. The energy addition due to combustion is determined in consideration of a single step, irreversible, global reaction between the fuel vapor and oxygen following a finite rate chemistry as:

$$C_{16}H_{34} + 24.5O_2 \rightarrow 16CO_2 + 17H_2O \tag{9}$$

In this study, the reaction rates that appear as source terms in species transport equation (Eq. (12)) are computed by using the eddy dissipation concept [4].

$$\dot{S}_j = A\rho\frac{\varepsilon}{k}\min[m_F s_F, m_{Ox}] \tag{10}$$

Here, m_F and m_{Ox} are fuel and oxygen mass fractions, respectively. s_F is the stoichiometric coefficient of fuel. Also, k and ε are turbulent kinetic energy and turbulent energy dissipation rate.

The gas phase equations are completed by the following equation of state which determines the distribution of density:

$$\rho = \frac{P}{RT}\left[\sum\frac{m_j}{M_j}\right] \tag{11}$$

Here, m_j and M_j are mass fraction and molecular weight of the j th species, respectively. This assumption is appropriate since the high temperatures associated with combustion generally results in sufficiently low densities for ideal gas behavior to be a reasonable approximation.

Individual species conservation:

$$\frac{1}{r}\left[\frac{\partial}{\partial x}(r\rho u m_j) + \frac{\partial}{\partial r}(r\rho v m_j)\right] = \Gamma_{mj}\nabla^2 m_j - \frac{1}{r}\frac{\partial}{\partial r}(r\rho\overline{v'm_j'}) - \frac{\partial}{\partial x}(\rho\overline{u'm_j'}) + \dot{S}_j \tag{12}$$

Here, $\dot{S}_j$ is the source term of the j th species.

In this study, species conservation equation is solved for fuel vapor, oxygen, carbon-dioxide and soot. The conservation equation for each species contains a source term related to the chemical reaction, which is negative for fuel vapor and oxygen but positive for carbon-dioxide. The equation for fuel vapor contains an additional source term to take care of the fuel mass evaporated from the droplets. The influence of soot formation and combustion on, respectively fuel and oxygen mass fractions is accounted for by a sink term added to the conservation equation of each of these species. A source term due to soot combustion is added to the CO_2 conservation equation.

Soot Formation

Two competing Phenomena exist in the soot process which are soot formation and soot combustion. In this study each phenomena is modeled separately.

A soot formation model, widely cited in literature, is the model proposed by Khan and his co-workers [5] which computes the rate of soot formation from an Arrhenious-type equation. This model was firstly introduced in diesel engines application and has been successfully used for other types of flames. To calculate soot mass fraction distribution, a transport equation must be solved. Source term for this equation is the net rate of soot generation and is given by,

$$\dot{S}_S = \dot{S}_{S,F} - \dot{S}_{S,C} \tag{13}$$

Here, the rate of soot formation is,

$$\dot{S}_{S,F} = C_s\phi^r P_F \exp(-E/RT) \tag{14}$$

And the rate of soot combustion (oxidation) is calculated by the Magnussen and Hjertager model [4]:

$$\dot{S}_{S,C} = A\rho\frac{\varepsilon}{k}\min\left[m_S, \frac{m_O}{s_S}\frac{m_S s_S}{m_S s_S + m_F s_F}\right] \tag{15}$$

Another well known model is the model proposed by Edelman and his co-workers [6] which is a modified version of the Khan's model for the prediction of soot formation inside gas turbine combustors. Using this model, source term for soot mass fraction transport equation is calculated similar to Eq. (13). Here, the rate of soot formation is,

$$\dot{S}_{S,F} = C_s T^a m_F^b m_{Ox}^c \rho^{b+c}\exp(-E/RT) \tag{16}$$

And the soot combustion rate ($\dot{S}_{S,C}$) is given by Eq. (15).

A more involved model commonly used in the majority of CFD commercial codes is proposed by Tesner et al. [7] which is based on kinetic theory of soot formation. The model assumes that soot forms in two-stages, where the first stage represents the formation of radical nuclei, and the second stage represents soot formation from these nuclei. Thus, two transport equations must be solved in this model, one equation for nuclei and the second for soot. Source term for nuclei transport equation is the net rate of nuclei generation and is given by,

$$\dot{S}_N = \dot{S}_{N,F} - \dot{S}_{N,C} \tag{17}$$

Where, the rate of nuclei formation depends on spontaneous formation and branching processes, describing by,

$$\dot{S}_{N,F} = \eta_0 + \rho\left[(F-G)m_N - \lambda_0 \rho m_N m_S\right] \tag{18}$$

Here, the rate of spontaneous generation of nuclei is,

$$\eta_0 = A_0 \rho \; m_F \exp(-E/RT) \tag{19}$$

The rate of nuclei combustion is assumed to be proportional to the rate of soot combustion:

$$\dot{S}_{N,C} = \dot{S}_{S,C} \frac{m_N}{m_S} \tag{20}$$

Where the soot combustion rate ($\dot{S}_{S,C}$) is given by Eq. (15).

Also, the source term for soot transport equation ($\dot{S}_S$) is calculated similar to Eq. (13). The rate of soot formation from the generated nuclei is calculated as,

$$\dot{S}_{S,F} = \rho M_p (\alpha - \beta \rho m_S) m_N \tag{21}$$

Where, the rate of soot combustion is calculated similar to Eq. (15).

As can be seen soot formation is described simply in terms of fuel concentration and temperature distributions showing that the major difference between the models corresponds to different relative roles of these two key parameters. Table 1 represents the constants used for theses models. In this study, the three soot models are adopted directly without any adjustment.

The effect of soot, which is usually the dominant radiating species in hydrocarbon-fueled flames [8], on the radiative heat transfer inside the combustor is accounted for by using a modified absorption coefficient (a) of the gas as:

$$a_m = a + b_1 \rho m_S \left[1 + b_T (T - 2000)\right] \tag{22}$$

Here, b_1 and b_T are empirical constants.

Table 1- Constants used for soot models.

Khan's single-step model	Edelman's single-step model	Tesner's two-step model
$C_s = 1.5$ $E/R = 20000K$ $r = 3$	$C_s = 4.66 \times 10^{14}$ $a = -1.94$ $E/R = 32000$ $b = 1.81$ $c = -0.5$	$\alpha = 10^5 \, part^{-1} s^{-1}$ $\beta = 8 \times 10^{-14} \, m^3 part^{-2} s^{-1}$ $(F-G) = 10^2 \, s^{-1}$ $A_0 = 6.4 \times 10^{30} \, s^{-1}$ $\lambda_0 = 10^{-15} \, m^3 part^{-1} s^{-1}$ $E/R = 90000K$

2-2-2- Generation of droplet phase information

The velocity, mass and temperature history of all droplet groups along their trajectories are obtained from the respective conservation equations on a Lagrangian frame similar to Sharma and Dom [9]:

Droplet velocity:

$$\frac{du_i^d}{dt} = \frac{3\mu C_D \, \mathrm{Re}_D}{4\rho_p D_p^2}\left(u_i^g - u_i^d\right) \tag{23}$$

Here, u_i^d is droplet velocity. Re_D is Reynolds number based on the droplet diameter (D_p). Also, ρ_p is droplet density. The drag coefficient (C_D) is computed following the standard drag law as given by Hinds [10]. Also, the effect of gas phase turbulence on the droplet motion is simulated using a stochastic approach [9].

Droplet mass:

$$\frac{dm^p}{dt} = -\pi \rho_p{}^2 D_p{}^2 \beta (m_{F,s} - m_F) \tag{24}$$

Here, m^p is the droplet mass. β is mass transfer coefficient. m_F is fuel vapor mass fraction and $m_{F,s}$ is fuel vapor mass fraction at the droplet surface.

Droplet temperature:

$$m^d c_p^d \frac{dT^d}{dt} = \pi d^2 h (T - T^d) + \frac{dm^d}{dt} \Delta H_v \tag{25}$$

Where, c_p^d is the droplet specific heat, T^d is droplet temperature, T is gas phase temperature, and h is heat transfer coefficient. Also, ΔH_v is the enthalpy of vaporization of the liquid fuel at the droplet temperature and heat transfer coefficient and mass transfer coefficient in Eqs. (24) and (25) respectively, are evaluated from:

$$Sh = \frac{2 + 0.6\,\mathrm{Re}_d^{0.5}\, Sc^{0.33}}{1 + B} \tag{26}$$

$$Nu = \frac{2 + 0.6\,\mathrm{Re}_d^{0.5}\, \mathrm{Pr}^{0.33}}{1 + B} \tag{25}$$

Here, Nu and Sh are Nusslet and Sherwood numbers. Also, Pr and Sc are Prandtl and Schmidt numbers and B is the transfer number. Eqs. (23), (24) and (25) are solved for V_i^d , m^d , and T^d respectively, with appropriate initial conditions.

The initial droplet size distribution of liquid fuel spray is assumed to follow the Rosin-Rammler distribution function given by,

$$G'(d_i) = \frac{\exp(-b d_i^n) - \exp(-b d_{\max,i}^n)}{\exp(-b d_{\min,i}^n) - \exp(-b d_{\max,i}^n)} \tag{26}$$

Where, $G'(d_i)$ is the mass fraction of the spray droplets having diameter above d_i . The dispersion parameter (n) is taken as used by Saario et al. [11].

Due to Faeth [12], ten droplet group sizes ranging from 50 to 120 μm are assumed for the calculation in the present model.

3- Method of solution

3-1- Numerical scheme

The gas conservation equations are solved using a control-volume based computational procedure [13]. The convective terms are discretized by the power law scheme. Pressure linked equations are solved by the SIMPLE algorithm and the set of algebraic equations are solved sequentially with the line-by-line tridiagonal-matrix algorithm. The convergence criteria employed is determined by the requirement that the maximum value of the normalized of any equation must be less than 1×10^{-5}. Under-relaxation factor is chosen as 0.3 for all dependent variables expect nuclei and soot, for which 0.4 is suitable. As in the previous work [14] this solution procedure has been modified for spray penetration and combustion, this paper concentrates on developing it for soot formation and combustion.

3-2- Numerical mesh

A numerical mesh of 120×68 grid nodes is used after several experiments, which shows that further refinement in either direction does not change the result (maximum difference in velocity and other scalar functions in the carrier phase) by more than 2%. The grid spacings in axial and radial directions are changed smoothly to minimize the deterioration of the formal accuracy of the finite difference scheme due to variable grid spacing and in such a way that a higher concentration of nodes occurs near the inlet and the walls.

3-3- Operating parameters and boundary conditions

Because of elliptic nature of the conservation equations, boundary conditions are specified at all boundaries of the domain considered. The air enters the combustor with an axial velocity equal to 18 m/s. Swirl number of the inlet air is considered as:

$$Sw = \frac{\int_{r_1}^{r_2} 2\pi\rho uwr^2 dr}{r_2 \int_{r_1}^{r_2} 2\pi\rho u^2 r dr} = 1.24 \qquad (27)$$

In this study, different inlet air temperatures are investigated. The k and ε profiles are specified using uniform distributions corresponding to a free stream turbulence intensity of $T_u = 5\%$. The liquid fuel is injected at 300 K and axially with a pressure-swirl atomizer in such a way that its axial velocity is 20 m/s and its tangential velocity is 14 m/s. Different equivalence ratios are investigated by testing different fuel flow rates. A zero axial gradient is prescribed at the outlet for all variables. Also, different temperatures are specified on the combustors walls.

4- Results and discussion

Numerical calculations are performed for a spray combustor of internal diameter 0.153 m and length 0.338 m. The computational procedure is first used to simulate the condition at which, inlet air temperature equals to 800 K. Fuel flowrate is determined in such a way that equivalence ratio be at 0.5. Temperature of the walls is assumed to be at 1200K . Also, size range of the fuel droplets in spray is chosen to be in the range of 50 to 120 μm .

Figs. 1 and 2 show the distribution of gas phase velocity field and temperature contours within the spray combustor for the specified condition from the solution of the present numerical model. It is observed from Fig. 1 that an internal recirculation zone (IRZ) has been established near the central axis upstream the combustor. That is due to the incoming swirling flow. Sudden expansion at the inlet also has established a corner recirculation zone near the walls. Presence of the internal recirculating flow helps to stabilize the flame near the axis close to the burner as evident from the high temperature contours shown in Fig. 2. The flame spreads in the radial direction in the primary zone depending mainly upon the cone angle of the spray.

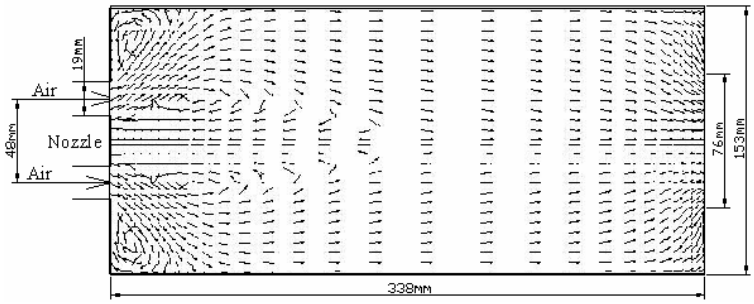

Fig. 1- Gas phase velocity field in the combustor.

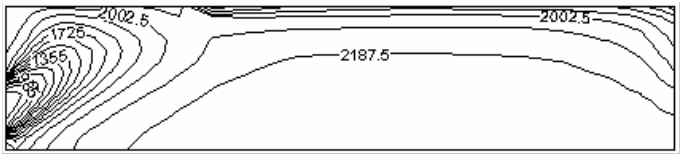

Fig. 2- Temperature (K) contours in the upper half of the combustor.

The accuracy of the quantitative or even the qualitative trends of the results relating to the combustion parameters depends on the accuracy with which velocity, temperature, and species concentration fields are determined from the numerical computation of the present model. To establish the accuracy of the present computation, a possible comparison between velocities and temperature distributions predicted by this model has been made with the experimental work of Khalil [15] under a similar condition. It is observed that predictions of axial and tangential velocity components agree fairly well with the experimental results (Fig. 3). The discrepancy between the two results can be due to turbulence modeling which shows that further works can be applied to the turbulence modeling. Similar trends can be observed from comparison between the temperature distribution

predicted by this model and the experimental results (Fig. 4). Discrepancy can be attributed to the fundamental assumption made in the combustion model used (Magnussen and Hjertager model [14]) which relates the rate of combustion with turbulent energy and dissipation.

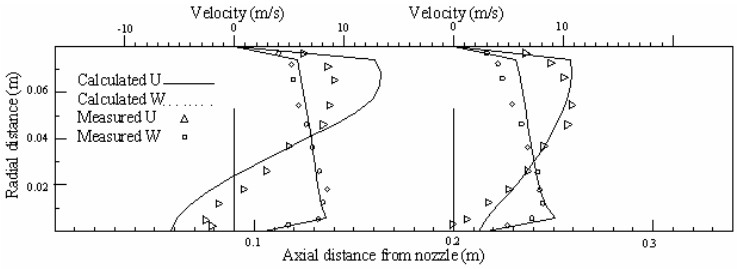

Fig. 3- Comparison of predicted axial and tangential velocity distributions with the experimental data.

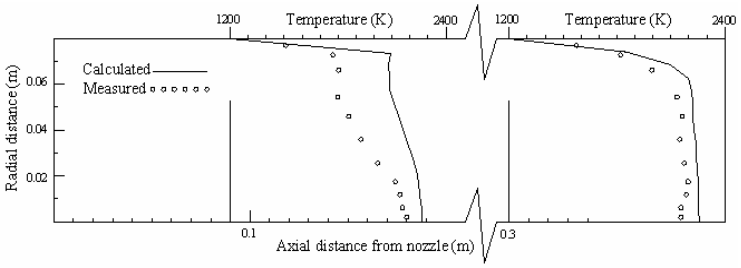

Fig. 4- Comparison of predicted axial and tangential velocity distributions with the experimental data

Fig. 5 shows the trajectories of individual evaporating droplets in the upper half of the combustor. It is seen that the smallest sizes evaporate completely in the vicinity of the point of issue whereas it takes time for larger droplets to heat up, reach the boiling point, and vaporize completely. Thus, larger fuel droplets penetrate longer axial distances in the combustor. Also, some of the droplets may be so large that they hit the cylindrical wall of the combustor before they vaporize completely [14].

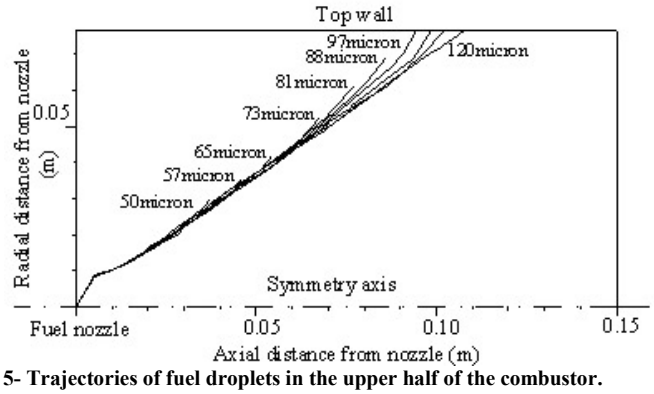

Fig. 5- Trajectories of fuel droplets in the upper half of the combustor.

Fig. 6 represents the centerline distributions of fuel vapor and temperature inside the combustor. The figure demonstrates that near the point of the issue, fuel vapor mass fraction attains a maximum and then decreases sharply due to combustion. The result could be expected from Fig. 5. Moving downstream, combustion of fuel is progressing and temperature increases quickly.

The distributions of soot predicted by the three soot models are shown in Fig. 7. The figure shows that the single-step models compute maximum soot mass fraction in the vicinity of the point of the issue where normally it is expected [16-18]. The two-step model behaves completely different. This discrepancy is due to the type of flame in which the two-step model has been derived (laminar diffusion flame). In contrast to turbulent flames which are mainly affected by turbulent mixing, gradient of fuel concentration is low inside laminar flames. Thus, the two-step model has been derived in a situation where the rate of soot formation was not markedly influenced by the fuel concentration. As a result, the two-step model is not so sensitive to the gradient of fuel concentration.

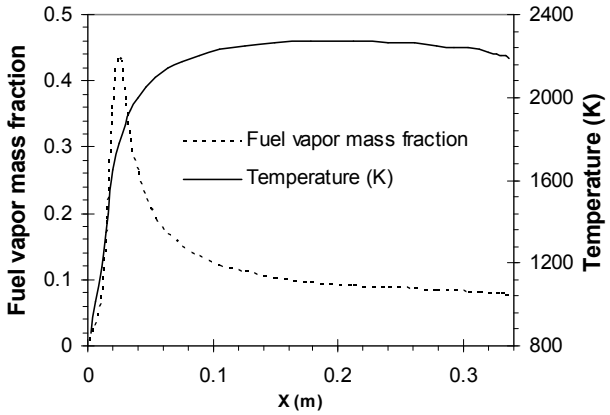

Fig. 6- Centerline distribution of fuel vapor mass fraction and temperature along the combustor

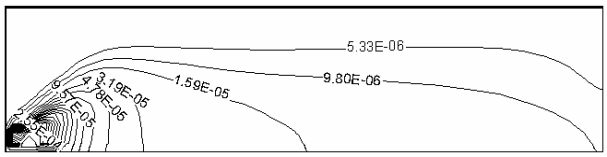

(a) Khan's single-step model.

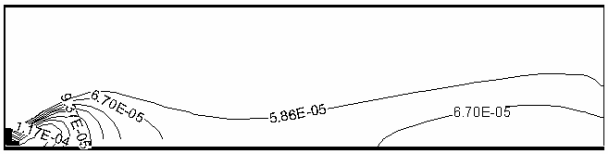

(b) Edelman's single-step model.

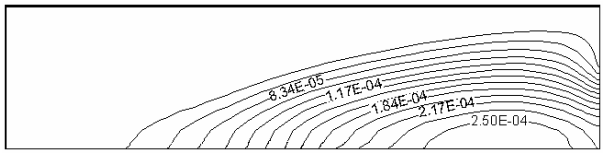

(c) Tesner's two-step model.

Fig. 7- Distributions of soot mass fraction inside the combustor predicted by the three soot models.

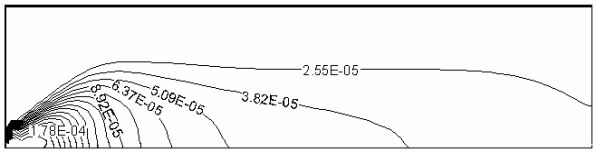

Fig. 8- Distributions of soot mass fraction inside the combustor predicted by the modified two-step model.

As we know, fuel plays an important role in the process of soot formation. In fact, it is fuel which leads to soot and its role must be correctly included. Thus, in this study the two-step model is modified to increase the accuracy of soot prediction. Modification is implemented by increasing the exponent of fuel vapor mass fraction in the process of nucleation. As a result the modified two-step model computes the rate of nucleation as:

$$\dot{S}_{N,F} = \eta_0 + \rho[(F-G)m_N - \lambda_0 \rho m_N m_S] \tag{28}$$

Where,

$$\eta_0 = A_0 \rho m_F^n \exp(-E/RT) \tag{29}$$

The modified model calculates the rate of soot formation from the generated nuclei similar to the original correlation:

$$\dot{S}_{S,F} = \rho M_p(\alpha - \beta \rho m_S) m_N \tag{30}$$

The value of the exponent (n) is increased from unity until the maximum soot zone computed by the model reaches to the other predictions in order to the role of fuel vapor concentration be correctly included. Result of the modified model is depicted in Fig. 8 which is in agreement with the predictions of the single-step models.

It is worth nothing that the weakness of the role of fuel concentration in the two-step model can be highlight only in the situations where the high temperature zone and the high fuel concentration zone are clearly distinct. It is clear from the conclusion that in such a situation, the weakness of the role of fuel vapor concentration leads to maximum soot concentration zone be predicted near the high temperature zone. The flame studied here includes such a character. In fact, as it is depicted in Fig. 6, in the vicinity of the point of the issue, the flame is fuel-rich while the high temperature zone is located upstream of the combustor.

Fig. 9 compares the predictions of the two-step model and the modified model inside the combustor against measurements of Prado et al. [18]. Note that different scales are used for the predictions and the experimental data. The good qualitative agreement of the modified model predictions with the experimental results confirms the modification. It is worth noting that in this study absolute value of soot formation is not considered. On the other hand, trends and behavior of soot prediction is investigated. Some constants in the models can be easily optimized to cater absolute values of soot formation if a set of experimental data can be available.

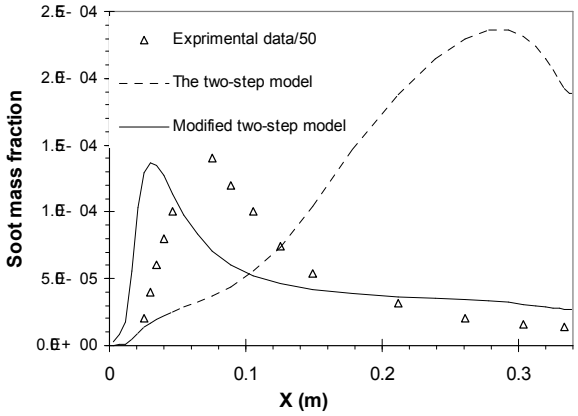

Fig. 9- Comparison between predictions of the two-step and the modified two-step models.

Fig. 10 compares the predictions of the modified two-step model and the single-step ones inside the combustor. Result of the Khan's model is concentrated in the vicinity of the point of the issue and it decreases rapidly, a pattern which is similar to the fuel vapor mass fraction (Fig. 6). This pattern is calculated since the model has been proposed in the studies on diesel engines where flames are generally fuel-lean and fuel concentration is the dominant parameter on the rate of soot formation. This demonstrates that the contribution of fuel concentration has become exaggerated in the Khan's model. The result of the Edelman's model is much more uniform. It also slightly increases downstream of the combustor. Such a pattern in soot prediction goes back to the conditions in which the Edelman's model has been proposed. In fact, the model has been obtained in the studies on gas turbine combustors where, as a result of inlet air staging, most of the flame is fuel-rich. Thus, in the process of soot formation in the studies of Edelman and his co-workers, fuel has not been a significant parameter. As a result, the role of fuel concentration is less influencial than temperature on this model. Strong dependence to temperature in the Edelman's model causes that, increase in temperature raises the prediction downstream of the combustor where a considerable reduction occurs in the fuel concentration. In contrast to these two models, prediction of the modified model is concentrated neither upstream of the combustor nor downstream of it. This matter demonstrates that contributions of temperature and fuel concentration are correctly included in the modified model and it is not too sensitive to none of them.

Behavior of the soot models under different equivalence ratios are depicted in Fig. 11. Parameter chosen to study in the figure is soot emission which defines as the mass fraction of soot in the outgoing gases. As it clear from the figure, all the models predict a low soot emission under fuel-lean condition while discrepancies increase with equivalence ratio. Here, prediction of the Edelman's model and the Tesner's model remain low under all equivalence ratios but the Khan's model results approaches to infinity near overall stoichiometric condition. The low value predictions are due to the weak role of fuel concentration in the corresponding models which was concluded before. The unrealistic prediction of the Khan's model near overall stoichiometric flame is a result of the strong role of fuel concentration in the model. In fact, using equivalence ratio term instead of fuel mass fraction term in the Khan's model equation (Eq. 14) significantly highlights the role of fuel concentration

on soot formation in such a way that soot prediction approaches to unity near overall stoichiometric flame. Thus, the Khan's model can not be implemented for the flames in which a region of flame includes only fuel, i.e. jet diffusion flames. As it is clear from the figure, the modified two-step model behaves as the most appropriate soot model under different equivalence ratios. This matter again confirms that contributions of temperature and fuel concentration are correctly included in the modified model. In addition, the modified model is capable to predict soot formation under a broad range of equivalence ratio, in contrast to the Khan's model.

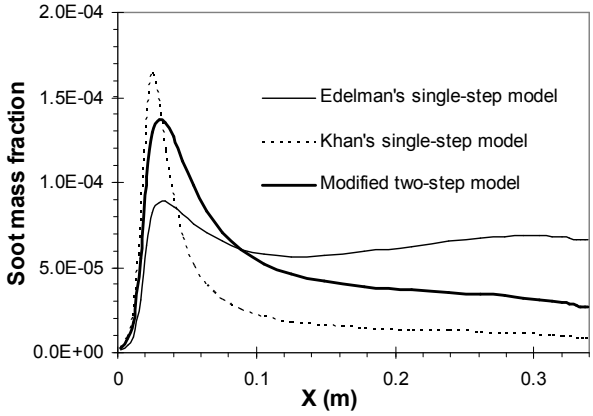

Fig. 10- Comparison between predictions of the single-step and the two-step models.

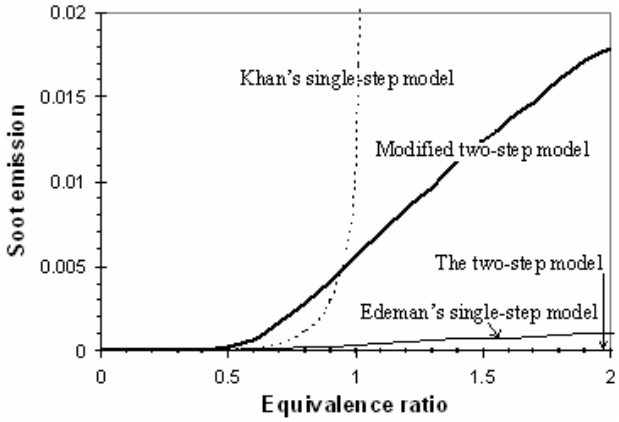

Fig. 11 Comparison between predictions of various soot models under different equivalence ratios.

5- Conclusion

A numerical simulation of soot process has been adopted to compare the relative roles of fuel concentration and temperature distributions in the prediction of three widely used single-step and two-step soot formation models. The single-step models calculate soot formation in just one step while the two-step model assumes that soot is formed in two-stages, where the first stage represents the formation of nuclei radicals, and the second stage represents soot formation from these nuclei. Along all the models, soot combustion has been estimated by a finite rate combustion model with eddy dissipation concept. By increasing the role of fuel concentration in the soot formation rate equation, a new version of the two-step model has been proposed. Based on the presented results, it can be concluded that the role of fuel concentration is high in the Khan's single-step model. The results also reveals that in the Edelman's single-step model and the two-step model, the role of temperature in the process of soot formation are inadequately high. In addition, the proposed model produces the best agreement with experimental data.

References

[1] German A. E. and Mahmud T., "Modelling of non-premixed swirl burner flows using a Reynolds-stress turbulence closure", Fuel, Vol. 84, pp.583 -594, 2005

[2] Zhang J., Nieh S., and Zhou L., "A new version of algebraic stress model for simulating strongly swirling flows", Numerical Heat Transfer, Vol. 22, pp. 49 55, 1992.

[3] Gosman A. D. and Lockwood F. C., "Incorporation of a flux model for radiation into a finite difference procedure for furnace calculations", 14th Symposium (International) on Combustion, 1973
[4] Magnussen B. F. and Hjertager B. H., "Mathematical models of turbulent combustion with special emphasis on soot formation and combustion", 16th symposium (International) on Combustion, 1976
[5] Khan I. M. and Greeves G. A., "A method for calculating the formation and combustion of soot in diesel engines", in Heat Transfer in Flames, 1974
[6] Edelman R., Farmer R., and Wong E., "Modelling Soot emission in combustion systems", Particulate Carbon, Plenum Press,1981
[7] Tesner P. A., Snegiriova T. D., and Knorre V. G., "Kinetics of dispersed carbon formation", Combustion and Flame, p. 253, 1971.
[8] Wang L., Haworth D. C., Turns S. R., Modest M. F., "Interactions among soot, thermal radiation, and NO*x* emissions in oxygen-enriched turbulent nonpremixed flames: a computational fluid dynamics modeling study", Combustion and Flame, Vol. 141, pp 170–179, 2005
[9] Sharma N. Y. and Dom S. K., "Influence of fuel volatility and spray parameters on combustion characteristics and NOx emission in a gas turbine combustor", Applied Thermal Engineering, Vol. 24, pp. 885–903, 2004
[10] Hinds W. C., "Aerosol Science and Technology", Wiley, New York, 1999
[11] Saario A., Rebola A., Coelho P. J., Costa M., and Oksanen A., "Heavy fuel oil combustion in a cylindrical laboratory furnace: measurements and modeling", Fuel, Vol.84, pp.359 –369, 2005.
[12] Faeth G M, "Evaporation and combustion of sprays", Progress in Energy and Combustion Sciences, Vol. 9, pp.51-75, 1983.
[13] Versteeg H. K. and Malalaseke W., "An introduction to computational fluid dynamics- The finite volume method", Longman Scientific & Technical, 1996.
[14] Moghiman M. and Maneshkarimi M. R., "On the dependence of spray evaporation and combustion on atomization techniques", Iranian Journal of Science and Technology, Vol. 25, 2002
[15] Khalil E. E., "Modeling of furnaces and combustors", Cairo University Press, 1982.
[16] Melton T. R., Inal F., and Senkan S. M., "Effect of equivalence ratio on the formation of polycyclic aromatic hydrocarbons and soot in premixed ethane flames", Combustion and Flame, Vol. 121, pp 671-678, 2000
[17] Moghiman M., Greunberger T. M., Bowen P. J., and Syred N., "Dynamics of soot formation by turbulent combustion and thermal decomposition of natural gas", Combustion Science and Technology, Vol. 174, pp 67-86, 2002
[18] Prado G. P., Lee M. L., Hites R. A., Hoult D. P., and Howard J. B., "Soot and hydrocarbon formation in turbulent diffusion flame", 16th Symposium (International) on combustion, 1977